Journal of Applied Polymer Science

Effects of glucose-functionalized multiwalled carbon nanotubes on the structural, mechanical, and thermal properties of chitosan nanocomposite films

Shadpour Mallakpour,[1,2,3] Maryam Madani[1]

[1]Organic Polymer Chemistry Research Laboratory, Department of Chemistry, Isfahan University of Technology, Isfahan 84156-83111, Islamic Republic of Iran

[2]Nanotechnology and Advanced Materials Institute, Isfahan University of Technology, Isfahan 84156-83111, Islamic Republic of Iran

[3]Center of Excellence in Sensors and Green Chemistry, Department of Chemistry, Isfahan University of Technology, Isfahan 84156-83111, Islamic Republic of Iran

Correspondence to: S. Mallakpour (E-mail: mallak@cc.iut.ac.ir, mallak777@yahoo.com or mallakpour84@alumni.ufl.edu.full)

ABSTRACT: A series of multiwalled carbon nanotubes (MWCNTs) grafted by chitosan nanocomposite (NC) films were prepared by a direct blending process and solution casting method. In this study, we modified multiwalled carbon nanotubes with glucose (MWCNT–Gl) for this purpose, and the effects of MWCNT–Gl on the structural, mechanical, and thermal properties of chitosan films with different contents of MWCNT–Gl were investigated. The structure, thermal stability, and mechanical properties of the composite were examined by X-ray diffraction, Fourier transform infrared spectroscopy, field emission scanning electron microscopy, transmission electron microscopy, thermogravimetric analysis, and mechanical testing. The results indicate that the MWCNTs treated by glucose were dispersed well in the chitosan matrix, and the tensile properties of the NC films were improved greatly compared with neat chitosan. Also, with increasing MWCNT–Gl content, the crystalline nature of chitosan decreased. © 2015 Wiley Periodicals, Inc. J. Appl. Polym. Sci. **2015**, *132*, 42022.

KEYWORDS: biocompatibility; biodegradable; polysaccharides; thermogravimetric analysis (TGA)

Received 12 October 2014; accepted 25 January 2015

DOI: 10.1002/app.42022

INTRODUCTION

Chitosan is a linear amino polysaccharide composed of β-(1,4)-2-amino-2-deoxy-D-glucose. Chitosan is biocompatible, biodegradable, and nontoxic and shows widespread biological activities.[1–3] Chitosan is normally insoluble in common solvents. However, in diluted acidic (pH < 6) aqueous solutions, the free amino groups on the chitosan chains are protonated; this results in the dissolution of chitosan. In addition, because of the unique structure of chitosan, which is attributed to the presence of the hydroxyl and amino groups in repeating units, this polymer can be used in many applications, including food processing, drug delivery, biomedical products, and adsorbents for organic and inorganic pollutants.[4–7] However, the main disadvantages of chitosan are its solubility only in acid solutions and its poor mechanical properties compared to synthetic polymers. To overcome these problems, the fabrication of nanocomposites (NCs) with nanofillers were developed.[8]

Among different fillers, carbon nanotubes (CNTs) have attracted wide interest because of their unique structural, electrical, and mechanical properties, including excellent chemical stability, electrical conductivity, and good corrosion resistance.[9–11] Therefore, the preparation of polymer/CNT NCs can improve the polymer properties.[12,13] CNTs have frequently been used for the preparation of polymer blend membranes for filtration and gas separation,[14–17] pervaporation,[18,19] and membrane distillation.[20,21]

It is important that the performance and properties of NCs are extremely affected by the interfacial compatibility between the polymer and nanofillers. However, the dispersion and compatibility of CNTs in the polymer matrix due to π–π interactions and van der Waal's interactions are difficult.[22,23] Thus, the chemical modification of CNTs is necessary. Several kinds of organic molecules have been used for modification,[24] for example, amino acids,[25,26] isocyanates,[27] and different polymers.[28–30]

Recently, glucose was applied to the modification of CNTs.[31] Glucose, a monosaccharide, is the most important carbohydrate in biology. The cell uses it as a source of energy and as a metabolic intermediate.

In this article, we report a facile approach for preparing a hybrid composite of chitosan and modified multiwalled carbon nanotubes (MWCNT)s with glucose. The glucose provides interfacial compatibility between MWCNTs and the chitosan matrix. The hybrid composites were expected to have diverse properties because each component would contribute different chemical and physical properties. The main objective of this study was to investigate the effect of functionalized MWCNTs on the chitosan properties.

EXPERIMENTAL

Materials

Carboxyl-modified MWCNTs (diameter = 8–15 nm, length ≈ 50 mm, carboxyl content = 2.56 wt %, purity > 95 wt %), manufactured by a thermal chemical vapor deposition process, were purchased from Neutrino Co. (Tehran, Iran). A medium-molecular-weight chitosan powder with a weight-average molecular weight of 1.095×10^6 g/mol and degree of deacetylation (DD) of −85% was purchased from Aldrich Chemical Co. (Milwaukee, WI). D-Glucose, *N,N′*-carbonyl diimidazole (CDI), and glacial acetic acid were used as received without further purification and were purchased from Merck Chemical Co. (Germany).

Preparation of the Chitosan/MWCNT-Gl NC Composite Films

The MWCNTs were functionalized with glucose according to our previous works.[31] Briefly, 50 mg of MWCNTs was dispersed in 10 mL of freshly prepared aqueous solution of CDI (10 mg/mL) and stirred at room temperature for 2 h. Then, 100 mg of glucose was added to the solution. This solution was stirred at room temperature for 2 h and ultrasonicated for 1 h. The mixture was decanted to remove the solvent. Then, the MWCNTs were washed thoroughly with water, filtered, and dried *in vacuo* to give the multiwalled carbon nanotubes with glucose (MWCNT–Gl) product.

The chitosan/MWCNT-Gl (CMG) NC films were fabricated through a solution casting method. Chitosan (3.0 g) was dissolved in 15 mL of 2% acetic aqueous solution, stirred for 3 h at room temperature, and ultrasonicated for 30 min. Various amounts of MWCNT–Gl (3, 5, and 7 wt %) were dispersed in 5 mL of deionized water with stirring for 3 h, and ultrasonication was performed for at least 1 h to make sure that the MWCNT–Gl were dispersed homogeneously. The prepared MWCNT–Gl solution was then added to the chitosan solution to give CMG NC solution, which was stirred for 24 h. Then, the solution was ultrasonicated for approximately 1 h. This solution was cast into a Petri dish and allowed to dry at room temperature for 24 h.

Characterization

Fourier Transform Infrared (FTIR) Spectrometry. The stretching frequencies of the samples were examined by FTIR spectroscopy (Jasco-680, Japan). The vibrational transition frequencies were reported in the range 4000–400 cm^{-1}. The spectrum of MWCNT–Gl was obtained with KBr pellets. The spectra of the CMG NC films were attained as a thin film for FTIR analysis.

X-ray Diffraction (XRD) Analysis. The XRD patterns were recorded on a Philips X'Pert MPD with a copper target operating at current of 100 mA and a voltage of 45 kV with Cu Kα radiation ($\lambda = 0.1542$ nm) in the range 10–80° at a speed of 0.05°/min. For XRD studies, rectangular pellets for MWCNT–Gl and the cutting dried film prepared by compression molding were used.

Thermogravimetric Analysis (TGA). TGA was achieved by the use of a STA503 TA (Germany) with scan range from of 25 to 800°C under a constant heating rate of 20°C/min with a continuous argon flow. The NC films dried *in vacuo* at 100°C for 8 h to remove the residual solvent.

Morphological Characterization.. The dispersion morphology of the samples was characterized with field emission scanning electron microscopy (FESEM; Hitachi S-4160). The samples of chitosan and CMG NC films were cut into rectangular specimens and sputter-coated with gold layer. The samples were observed at accelerating voltages of 10 and 30 kV.

Atomic force microscopy (AFM) topographic images were evaluated with Nano S1/1 (Bruker, Germany, noncontact mode).

The ultrathin sections (30–80 nm) of MWCNT–Gl and the CMG NC were prepared with a Leica ultramicrotome. Then, transmission electron microscopy (TEM) images were obtained with a Philips CM 120 microscope with an accelerating voltage of 150 kV.

Tensile Measurements. Tensile testing was performed at room temperature on a Testometric universal testing machine M350/500 (United Kingdom) according to ASTM D 882 (standards). Tests were carried out with a crosshead speed of 12.5 mm/min. The dimensions of the test specimens were $35 \times 2 \times 0.04$ mm^3. The property values reported here represent an average of the results for tests runs on at least three specimens. The tensile strength, tensile modulus, and strain were obtained from these measurements.

RESULTS AND DISCUSSION

Preparation of the CMG NC Films

The dispersion of MWCNTs plays a very important role in the use of filler properties in chitosan NCs. The MWCNTs, because of their high surface area, tend to agglomerate greatly. This reduces their ability to show their expected properties. The chemical modification and ultrasonication of MWCNTs are techniques that are used to achieve their good dispersion in the polymer matrix. On the other hand, unlike MWCNTs, modified MWCNTs can increase their compatibility with the polymeric matrix and improve their dispersion ability.

In this study, we used carboxylated–MWCNT (MWCNT–COOH) for modification with biomolecules. The covalent modification of MWCNTs has been described in the literature and is mainly based on the attachment of material blocks to the carboxylic functions that are formed by the oxidation of CNTs with strong acids.[32] Therefore, MWCNT–COOH were modified with glucose in the presence of CDI. The CDI catalyzed an

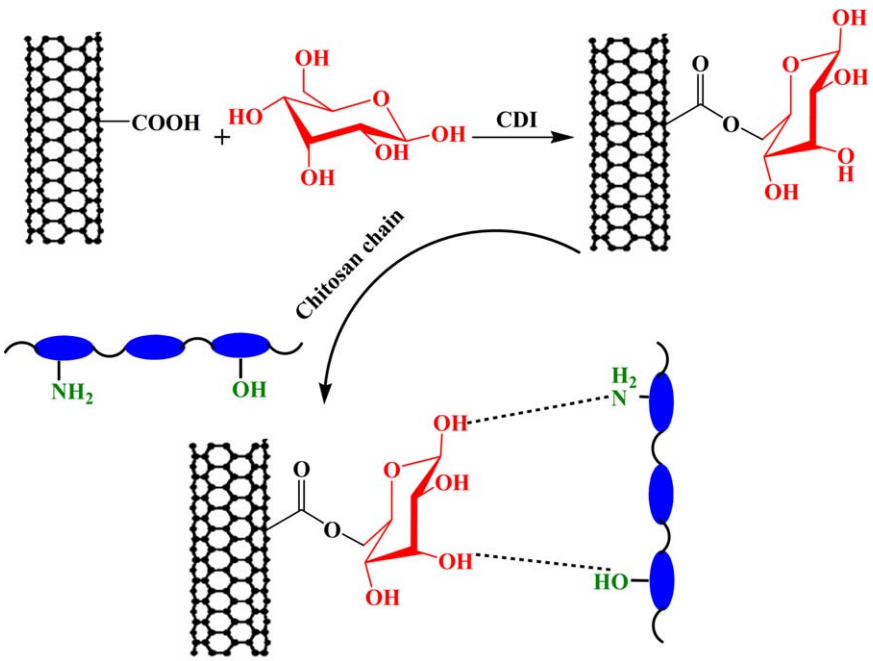

Scheme 1. Schematic illustration of the functionalization of MWCNTs and the preparation of CMG NCs. [Color figure can be viewed in the online issue, which is available at wileyonlinelibrary.com.]

esterification reaction between the carboxylic acid group of MWCNT–COOH and glucose molecules. Then chitosan/MWCNT–Gl NCs were prepared by the addition of 3, 5, and 7 wt % MWCNT–Gl in a chitosan solution via vigorous stirring for 24 h and utrasonication for 1 h. Scheme 1 shows the experimental steps involved in this chemical modification of MWCNT–COOH for the preparation of the CMG NC films and also possible interactions between the chitosan and MWCNT–Gl. Moreover, the amine and hydroxyl groups in the backbone of chitosan performed hydrogen bonding with the modified CNTs, and a composite based on hydrogen bonding was fabricated.

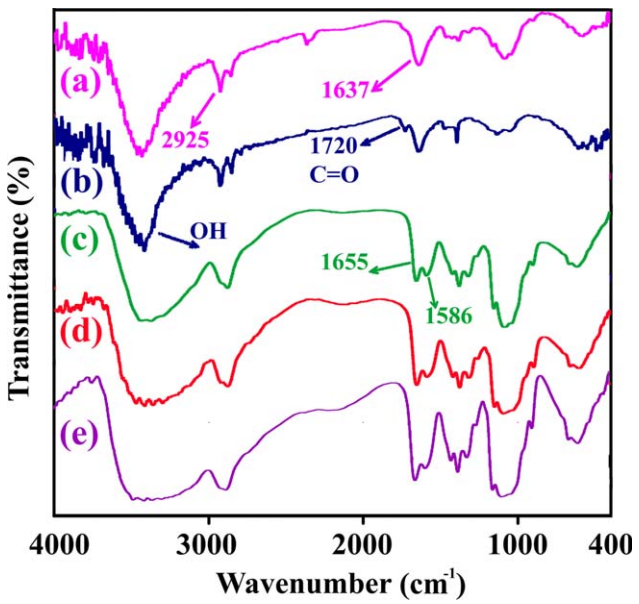

Figure 1. FTIR spectra of the (a) pure chitosan, (b) MWCNT–Gl, (c) 3 wt % CMG NCs, (d) 5 wt % CMG NCs, and (e) 7 wt % CMG NCs. [Color figure can be viewed in the online issue, which is available at wileyonlinelibrary.com.]

FTIR Spectra

The interactions of MWCNT–Gl with the chitosan matrix were analyzed by FTIR spectroscopy, as presented in Figure 1. In the spectrum of chitosan [Figure 1(a)], the characteristic bands at 3450 cm^{-1}, due to the stretching vibrations of —OH overlaid on the —NH stretching band, broadened because of the interhydrogen bonds of chitosan. The characteristic absorption bands appearing at 1637 cm^{-1} were ascribed to the amide group (C═O stretching). The peak at 1419 cm^{-1} was ascribed to the —C—O stretching of the primary alcoholic group in chitosan, and that at 1080 cm^{-1} was attributed to C—O—C stretching vibrations. In the spectrum of MWCNT–Gl [Figure 1(b)], the band at 3449 cm^{-1} was attributed to the stretching vibrations of O—H bond. The characteristic bands at 2927 and 1720 cm^{-1} were attributed to the —CH stretching vibrations and —COO groups, respectively. In the spectrum of the CMG NCs [Figure 1(c–e)], the peaks at 3400 and 1637 cm^{-1} were attributed to the stretching vibrations of —OH and C═O stretching.

Crystallinity

The difference in the crystallinity between chitosan and the CMG NCs were analyzed with XRD measurements. The XRD results of the pure chitosan, CMG NCs, and MWCNT–Gl are shown in Figure 2. Ogawa *et al.*[33] proposed three forms for chitosan: noncrystalline, hydrated (tendon) crystalline, and anhydrous (annealed) crystalline. The hydrated polymorph showed a strong equatorial reflection spot at a 2θ of around 10°, and the anhydrous crystalline structure gave a strong spot around 15°. The diffraction pattern of the pure chitosan had characteristic peaks at 2θs of 10 and 20.93°. This peak was shown that the

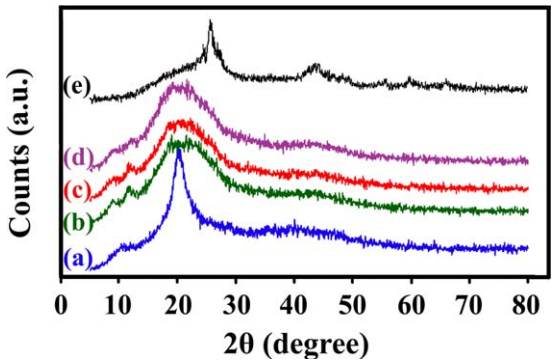

Figure 2. XRD patterns of the (a) pure chitosan, (b) 3 wt % CMG NCs, (c) 5 wt % CMG NCs, (d) 7 wt % CMG NCs, and (e) MWCNT–Gl. [Color figure can be viewed in the online issue, which is available at wileyonlinelibrary.com.]

chitosan was hydrated crystals.[34] In the hydrated chitosan crystals, adjacent chitosan chains were aligned antiparallel and bonded with intermolecular hydrogen bonding, forming a sheet structure. Furthermore, several sheets were stacked together with hydrogen bonding via water molecules present between them to form 3-D crystals.[35]

The XRD patterns of the CMG NCs appeared the characteristic peaks of the pure chitosan [Figure 2(b–d)]. However, this peak in the CMG NCs was weaker than that of pure chitosan; this indicated that the MWCNT–Gl expanded the spacing between chitosan chains in each sheet. This might have been due to possible interaction between the amino groups of chitosan and the functional groups in MWCNT–Gl. Therefore, the crystallinity of the chitosan decreased with the addition of MWCNT–Gl.

For MWCNT–Gl [Figure 2(e)], peaks at 2θ angles of 26 and 44° were associated with the (002) and (100) diffractions, respectively, of the hexagonal graphite structure. The spectra of the CMG NCs did not show any distinct diffraction peaks corresponding to the MWCNTs ($2\theta = 26$ and 44°). This was due to the low concentration of MWCNTs and high intensity of the background.

TGA

The TGA curves of the MWCNT–COOH, MWCNT–Gl, chitosan, and CMG NC films are presented in Figure 3. As shown in

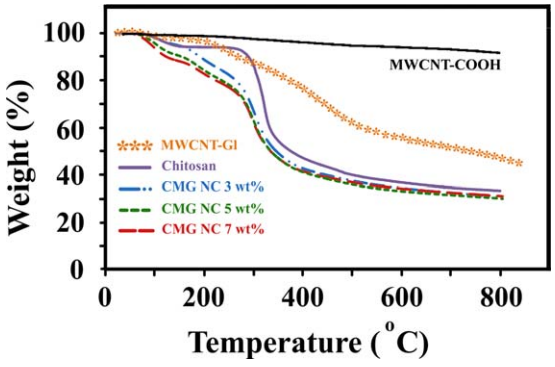

Figure 3. TGA curves of the pure chitosan and CMG NCs with different MWCNT–Gl contents. [Color figure can be viewed in the online issue, which is available at wileyonlinelibrary.com.]

Table I. TGA Results for the Chitosan and CMG NCs

Sample	T_{10} (°C)[a]	Residual mass (%)
Chitosan	288.6	33.5
CMG NC 3 wt %	190.2	30.9
CMG NC 5 wt %	154.3	30.7
CMG NC 7 wt %	122.1	31.1

[a] Recorded by TGA at a heating rate of 20°C/min under an argon atmosphere.

Figure 3, MWCNT–COOH were more stable and showed a small decomposition in the temperature range 0–550°C. According to previous reports, the TGA curves of glucose showed two decomposition processes: the first around 227°C, with a weight loss of 20%, which was related to dehydration, and the second around 337°C, with an approximately 65% weight loss, which was related to the decomposition of the stronger chemical bonds in glucose.[36] The weight loss of MWCNT–Gl was in the temperature range 230–700°C. This resulted from the decomposition of the glucose moieties attached to the surface of the MWCNTs.[29] As shown in graph, we could readily predict that the weight ratio of the grafted glucose onto the MWCNTs was around 32%. Ong *et al.*[37] used from the TGA for estimate the weight percentage of functionalized poly(3-hydroxybutyrate) (PHB) on the MWCNT.

Two stages of thermal degradation were found for the pure chitosan. The first weight loss region was at about 100–200°C and was due to the evaporation of water molecules or the volatilization of small molecules. The second stage of degradation ranged from 200 to 400°C and corresponded to a weight loss of 50–56%; this was attributed to the decomposition of chitosan, vaporization, and elimination of volatile products.[38] The thermal decomposition of the CMG NC films proceeded in two distinct stages. The temperature corresponding to a weight loss of 10 wt % (T_{10}) was selected for comparison and is listed in Table I. When the MWCNT–Gl were added, T_{10} shifted to a lower temperature than that obtained for the pure chitosan. Possible reasons for these results may have arisen from the following facts. Chitosan is a semicrystalline polymer. The crystalline structure of chitosan is mainly stabilized by hydrogen bonding between polymer chains. The interaction between the MWCNT–Gl and chitosan probably weakened the interchain interactions in chitosan and assisted the thermal degradation of chitosan. In the other word, MWCNT–Gl placed between chitosan chains in each sheet that interacted with the amino groups of chitosan chains deteriorated the intermolecular hydrogen bonding, and this could eventually lead to the tearing of chitosan crystalline. Also, the glucose attached to the MWCNTs decomposed in the range 227–337°C. Thus, the thermal stability of chitosan decreased with increasing MWCNT–Gl content and remarkably decreased T_{10}.

Finally, after the decomposition and degradation of materials, the residual weight of the CMG NCs followed the order for chitosan: 3, 5, and 7 wt % CMG NCs with values of 33.44, 30.89, 30.66, and 31.13%, respectively.

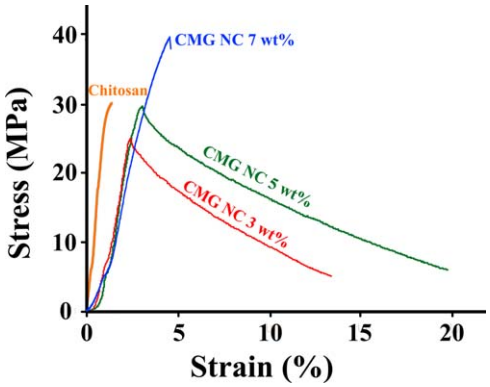

Figure 4. Mechanical properties of the pure chitosan and CMG NCs with different MWCNT–Gl contents. [Color figure can be viewed in the online issue, which is available at wileyonlinelibrary.com.]

Because of the high molecular weight (weight-average molecular weight = 1.095×10^6 g/mol), the thermal stability and especially the char yield did not increase. Because in the high-molecular-weight chitosan, the forces between the chitosan chains were strong. The interaction at the interface of chitosan and the modified MWCNTs weakened the forces of the chitosan interchains and assisted in the thermal decomposition of chitosan in the NC films. Also, perhaps groups attached to the MWCNTs were destroyed at low temperatures, and this helped to reduce the thermal stability of chitosan. Similar results were observed in Salam *et al.*'s[39] work, despite the greater amount of CNTs used. Perhaps if the molecular weight of chitosan was low, the MWCNTs could increase the thermal stability much more.[32]

Mechanical Properties of the CMG NCs

Figure 4 shows the representative tensile stress–strain curves of CMG NCs with various MWCNT–Gl contents. The results of the tensile mechanical tests of chitosan and CMG NC films are summarized in Table II.

The MWCNTs significantly enhanced the tensile strength because of their homogeneous dispersion in the polymer matrix. The tensile strength increased with increasing MWCNT–Gl content. However, the values of Young's modulus decreased for high values of MWCNT–Gl concentration. As shown in Figure 4, the chitosan was a rigid and brittle polymer that could withstand a good deal of stress, but it did not withstand much elongation before breaking. Also, the slope of the chitosan's plot was very steep; this means that it took a lot of force to deform. After the addition of MWCNT–Gl to the chitosan matrix, we expected an increase in the tensile strength of the NC films. The tensile strength and elongation of the 7 wt % CMG NCs were enhanced by 34 and 190%, respectively. These results reveal that the existence of MWCNTs in the chitosan matrix, their rigidity, and the high-aspect ratio of the MWCNTs effectively improved the flexibility of the NCs. The main reason could also be ascribed the better interfacial compatibility between the MWCNTs and the chitosan matrix. Also, the glucose had plasticizer properties, which could form hydrogen bonds with the functional groups of the chitosan chains.[40] By reducing the internal hydrogen bonding between the chitosan chains, we decreased the density of intermolecular interactions in the polymer chain and increased the free volume between the polymer chains. Thus, the incorporation of MWCNT–Gl decreased the tensile strength and Young's modulus but increased the tensile strength of the 7 wt % CMG NCs because the higher aspect ratio and interfacial area made the stress transfer to the graphite sheet more effective and, consequently, improved the mechanical properties of the formed NCs. The tensile strength of the NCs containing 3 wt % MWCNT–Gl was lower than that of the pristine chitosan, and that of the 5 wt % CMG NCs was similar to that of chitosan. However, the elongation increased compared with that of neat chitosan in all of the NC films. This result indicates that the CMG NC films were more flexible than that of chitosan.

Table II. Mechanical Properties of the Chitosan and CMG NC Films

Sample	Tensile strength (MPa)	Young's modulus (GPa)	Strain (%)
Chitosan	30.07	21.32	1.41
CMG NC 3 wt %	25.1	10.6	2.35
CMG NC 5 wt %	29.82	10.28	2.90
CMG NC 7 wt %	40.24	9.8	4.09

The CMG NC films with the better compatibility between the MWCNTs and the polymer matrix showed a greater reinforcement of the tensile strength. In addition, the existence of hydrogen-bonding interactions between the hydroxyl and amine groups of chitosan and the hydroxyl groups of the MWCNT–Gl resulted in enhanced interaction between the chitosan and MWCNTs with improved mechanical properties.[41]

Sun *et al.*[42] observed that functionalized CNTs as a reinforced filler for the chitosan matrix showed a significant improvement in their mechanical properties, and this noticeably enhanced the interfacial adhesion and reduced the brittleness of the porous materials.

Morphology Study

The morphology and distribution of the modified MWCNT were characterized with FESEM. Figure 5(a) shows the FESEM photos of MWCNT–Gl. These photos show a rough and debundled structure. This suggests that the MWCNTs were functionalized by glucose.

To provide more information on the morphologies, we investigated the modified MWCNTs further with AFM and TEM. Figure 5(b) shows the AFM photos of the one- and two-dimensional MWCNT–Gl. These photos clearly indicate that the MWCNTs had a cylindrical-shaped tubular morphology, and the walls were located side by side regularly. Shown in Figure 5(c) is a typical TEM image for the MWCNT–Gl sample with the estimated diameter of about 20–30 nm. These images indicate that the MWCNT–Gl were nanotubular in shape and had a high surface roughness.

The morphological features, cross section, and homogeneity of the composite of chitosan were analyzed through FESEM

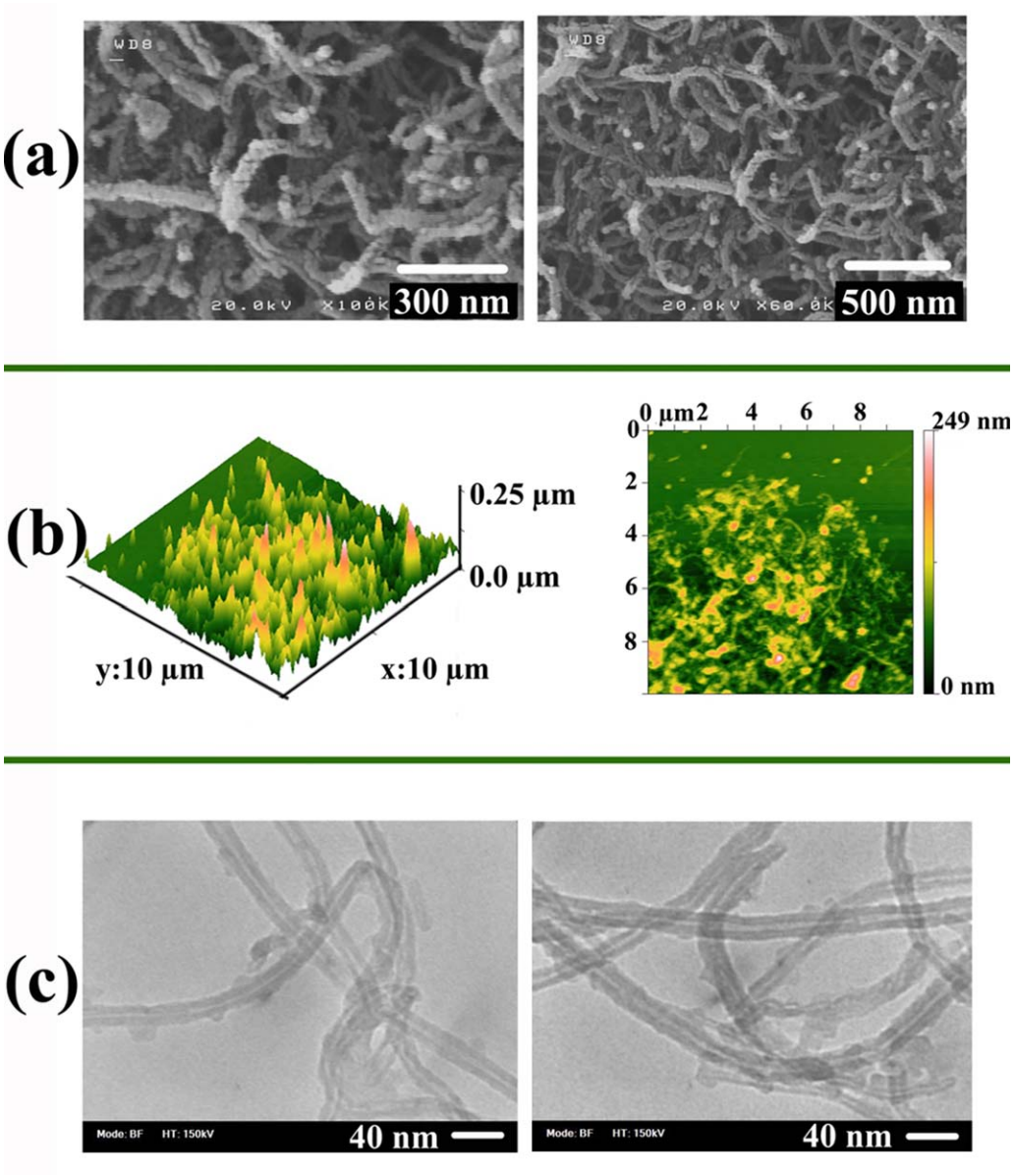

Figure 5. (a) FESEM micrographs of MWCNT–Gl at different magnifications, (b) AFM images of MWCNT–Gl, and (c) TEM micrographs of MWCNT–Gl at different magnifications. [Color figure can be viewed in the online issue, which is available at wileyonlinelibrary.com.]

analysis, as shown in Figure 6. The chitosan film [Figure 6(a,b)] showed a flat and smooth fracture surface, whereas the incorporation of MWCNT–Gl into chitosan matrix showed a uniform morphology, which was attributed to the good dispersion of MWCNT–Gl into the chitosan matrix, as shown in Figure 6(c–h). In Figure 6(c–h), the appearance of a white spot suggests some heterogeneity in the chitosan matrix when MWCNT–Gl were incorporated into chitosan. The observation that most of the MWCNTs were broken rather than pulled out from the chitosan matrix indicated a strong interfacial adhesion between the chitosan and MWCNT–Gl.[41]

Figure 7 shows the AFM and TEM images of the chitosan matrix and 7 wt % CMG NC surfaces. As shown in Figure 7(a), the presence of small bulges indicated that the chitosan was rather crystalline. After the addition of MWCNT–Gl into the chitosan, the morphology of the surface changed [Figure 7(b)]. The TEM images of the 7 wt % CMG NC are depicted in Figure 7(c). The uniformly dispersed black dots and lines that represent the ends of the MWCNT–Gl are shown in Figure 7(c).

CONCLUSIONS

A novel chitosan NC films reinforced with functionalized MWCNTs with glucose were successfully prepared by solution casting at room temperature. The interaction and hydrogen bonding between the chitosan and MWCNT–Gl were confirmed by spectroscopy and morphological analysis. The FTIR results indicate an enhanced hydrogen-bonding interaction between

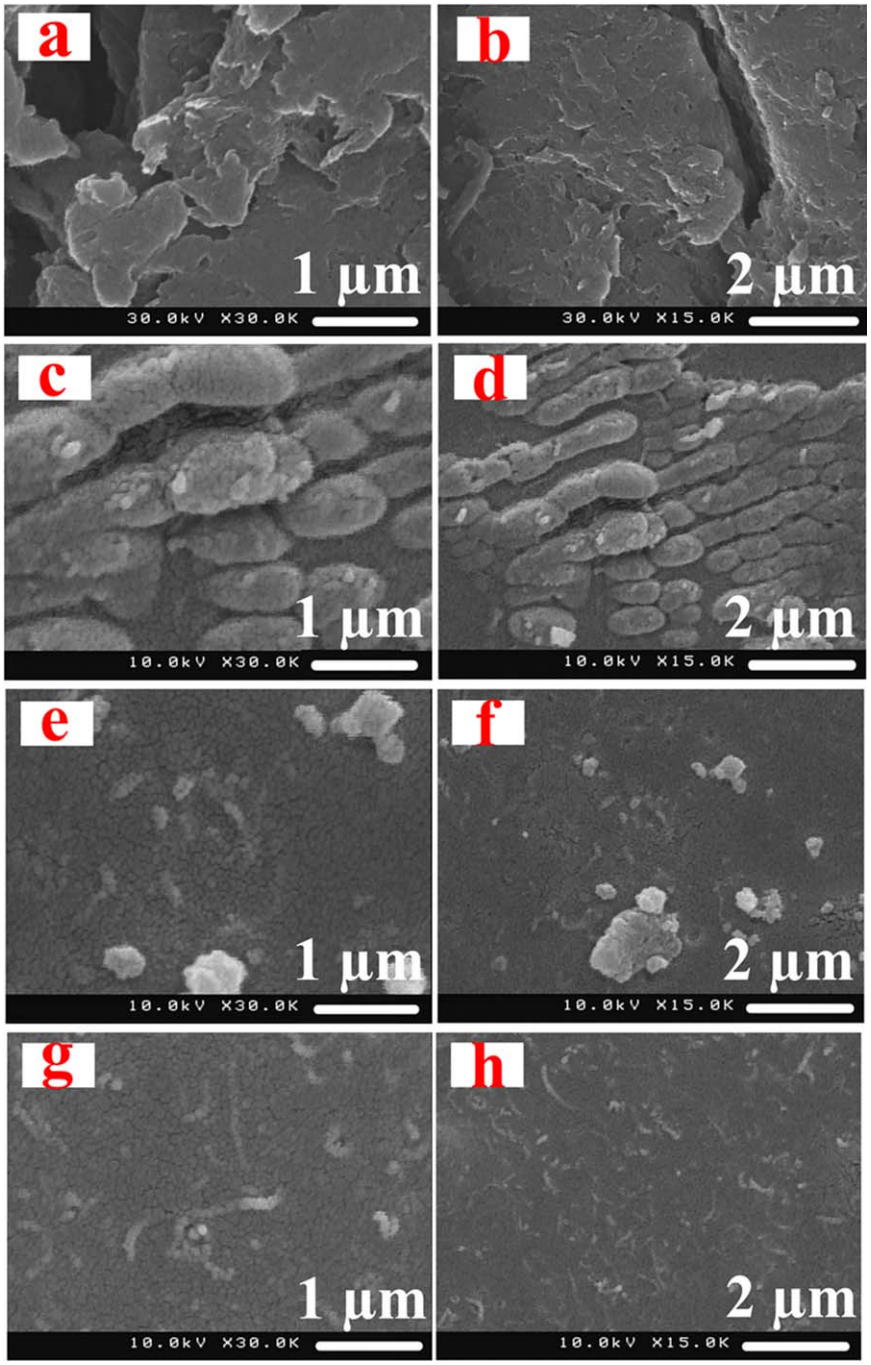

Figure 6. FESEM micrographs of the (a,b) pure chitosan, (c,d) 3 wt % CMG NCs, (e,f) 5 wt % CMG NCs, and (g,h) 7 wt % CMG NCs. [Color figure can be viewed in the online issue, which is available at wileyonlinelibrary.com.]

chitosan and MWCNT–Gl. In addition, the XRD analysis of CMG NC films showed that the crystallinity of chitosan was decreased. In the other word, the addition of different contents of MWCNT–Gl exhibited the formation of intermolecular hydrogen bonding between the functional groups of chitosan (amine and hydroxyl) and the hydroxyl groups of MWCNT–Gl. The TGA results suggest that the chitosan was slightly more thermally stable than the CMG NC films. This could be explained by the fact that the small amount of MWCNT–Gl could break the networks formed by chitosan chains via intermolecular/intramolecular interactions. The decreased intermolecular interactions of chitosan led to the slight decrease observed in the TGA. However, when the MWCNT–Gl loading increased in chitosan, the tensile strength and elongation of the CMG NCs were improved. The AFM, FESEM, and TEM results of CMG NC showed that the 7 wt % CMG NCs had a much rougher surface, and MWCNT–Gl could be uniformly dispersed in chitosan.

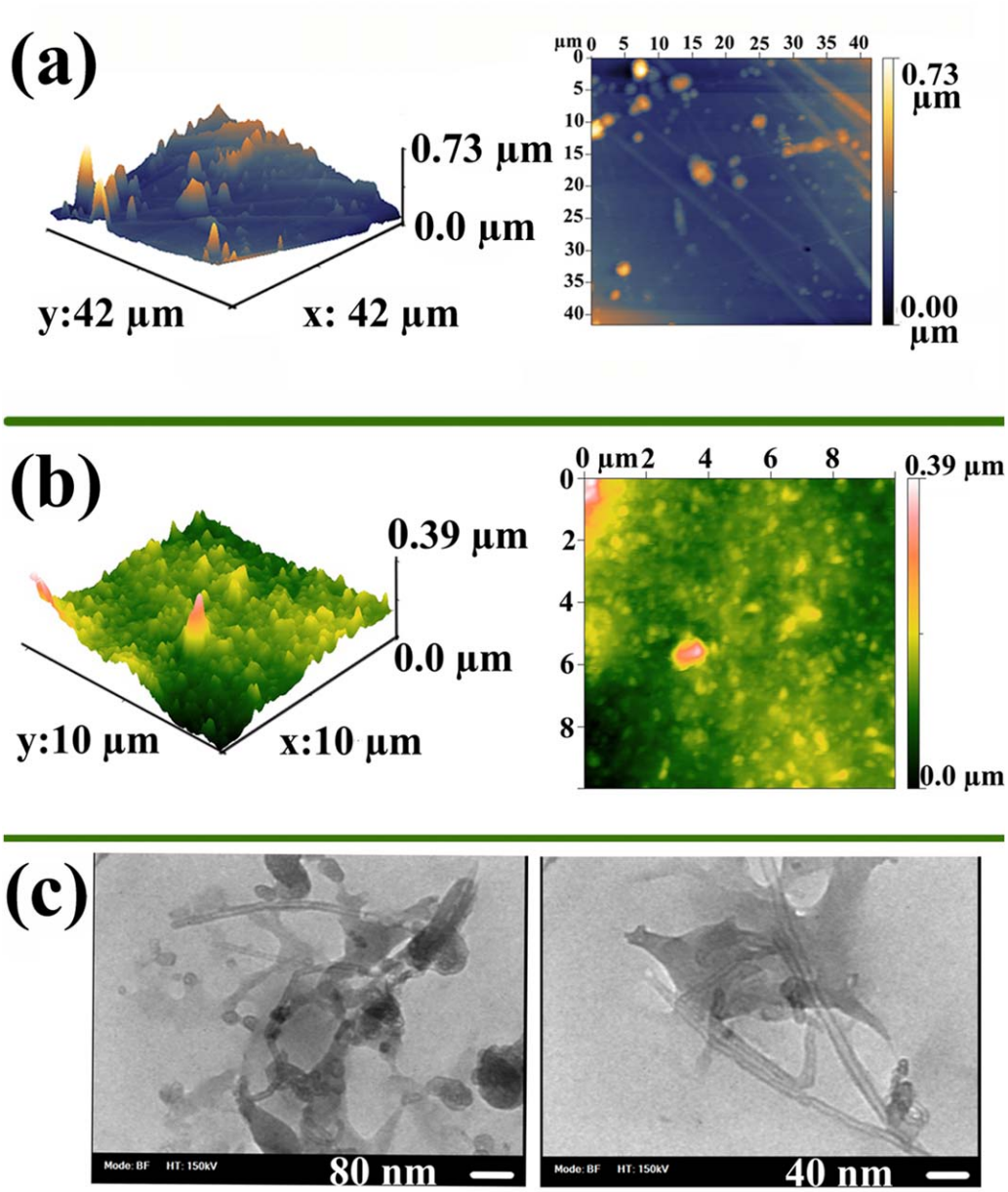

Figure 7. (a) AFM images of chitosan, (b) AFM images of 7 wt % CMG NCs, and (c) TEM images of 7 wt % CMG NCs at different magnifications. [Color figure can be viewed in the online issue, which is available at wileyonlinelibrary.com.]

ACKNOWLEDGMENTS

The authors thank the Research Affairs Division of Isfahan University of Technology, the National Elite Foundation, and the Center of Excellency in Sensors and Green Chemistry Research (Isfahan University of Technology) for their financial support.

REFERENCES

1. Muzzarelli, R. A. A. *Carbohydr. Polym.* **2009**, *76*, 167.
2. Rinaudo, M. *Prog. Polym. Sci.* **2006**, *31*, 603.
3. Mucha, M.; Wańkowicz, K.; Balcerzak, J. *e-Polymers* **2007**, *7*, 181.
4. Badawy, M. E. I. *J. Appl. Polym. Sci.* **2010**, *117*, 960.
5. Dash, M.; Chiellini, F.; Ottenbrite, R. M.; Chiellini, E. *Prog. Polym. Sci.* **2011**, *36*, 981.
6. Jayakumar, R.; Menon, D.; Manzoor, K.; Nair, S. V.; Tamura, H. *Carbohydr. Polym.* **2010**, *82*, 227.
7. Croisier, F.; Jérôme, C. *Eur. Polym. J.* **2013**, *49*, 780.
8. Chiu, F. C.; Lai, S. M.; Hsieh, I. C.; Don, T. M.; Huang, C. Y. *J. Polym. Res.* **2012**, *19*, 1.
9. Guo, G.; Yang, D.; Wang, C.; Yang, S. *Macromolecules* **2006**, *39*, 9035.
10. Popov, V. N. *Mater. Sci. Eng. Rep.* **2004**, *43*, 61.
11. Singh, B. K.; Kar, P.; Shrivastava, N. K.; Banerjee, S.; Khatua, B. B. *J. Appl. Polym. Sci.* **2012**, *124*, 3165.

12. Facca, S.; Lahiri, D.; Fioretti, F.; Messadeq, N.; Mainard, D.; Benkirane-Jessel, N.; Agarwal, A. *ACS Nano* **2011**, *5*, 4790.
13. Yang, X.; Tu, Y.; Li, L.; Shang, S.; Tao, X.-M. *ACS Appl. Mater. Interfaces* **2010**, *2*, 1707.
14. Roy, S.; Ntim, S. A.; Mitra, S.; Sirkar, K. K. *J. Membr. Sci.* **2011**, *375*, 81.
15. Wu, H.; Tang, B.; Wu, P. *J. Membr. Sci.* **2010**, *362*, 374.
16. Yu, B.; Cong, H.; Li, Z.; Tang, J.; Zhao, X. S. *J. Appl. Polym. Sci.* **2013**, *130*, 2867.
17. Lawrence Arockiasamy, D.; Alam, J.; Alhoshan, M. *Appl. Water. Sci.* **2013**, *3*, 93.
18. Amirilargani, M.; Tofighy, M. A.; Mohammadi, T.; Sadatnia, B. *Ind. Eng. Chem. Res.* **2014**, *53*, 12819.
19. Van der Bruggen, B. *ISRN Nanotechnol.* **2012**, *2012*, 17.
20. Dumée, L.; Germain, V.; Sears, K.; Schütz, J.; Finn, N.; Duke, M.; Cerneaux, S.; Cornu, D.; Gray, S. *J. Membr. Sci.* **2011**, *376*, 241.
21. Das, R.; Ali, M. E.; Hamid, S. B. A.; Ramakrishna, S.; Chowdhury, Z. Z. *Desalination* **2014**, *336*, 97.
22. Lee, H.-J.; Oh, S.-J.; Choi, J.-Y.; Kim, J. W.; Han, J.; Tan, L.-S.; Baek, J.-B. *Chem. Mater.* **2005**, *17*, 5057.
23. Song, Y. S.; Youn, J. R. *Carbon* **2005**, *43*, 1378.
24. Mallakpour, S.; Soltanian, S. *J. Polym. Res.* **2014**, *21*, 1.
25. Mallakpour, S.; Zadehnazari, A. *Synth. Met.* **2013**, *169*, 1.
26. Khan, M. A. K.; Kerman, K.; Petryk, M.; Kraatz, H.-B. *Anal. Chem.* **2008**, *80*, 2574.
27. Yoo, H. J.; Jung, Y. C.; Cho, J. W. *J. Polym. Sci. Part B: Polym. Phys.* **2008**, *46*, 900.
28. Salavagione, H. J.; Martínez, G.; Ballesteros, C. *Macromolecules* **2010**, *43*, 9754.
29. Golosova, A. A.; Adelsberger, J.; Sepe, A.; Niedermeier, M. A.; Lindner, P.; Funari, S. S.; Jordan, R.; Papadakis, C. M. *J. Phys. Chem. C* **2012**, *116*, 15765.
30. Zhang, F.-M.; Chang, J.; Eberhard, B. *New Carbon Mater.* **2010**, *25*, 241.
31. Mallakpour, S.; Zadehnazari, A. *Polymer* **2013**, *54*, 6329.
32. Carson, S.; Kelly-Brown, C.; Stewart, M.; Oki, A.; Regisford, G.; Luo, Z.; Bakhmutov, V. I. *Mater. Lett.* **2009**, *63*, 617.
33. Ogawa, K.; Yui, T.; Miya, M. *Biosci. Biotechnol. Biochem.* **1992**, *56*, 858.
34. Yen, M.-T.; Yang, J.-H.; Mau, J.-L. *Carbohydr. Polym.* **2009**, *75*, 15.
35. Okuyama, K.; Noguchi, K.; Miyazawa, T.; Yui, T.; Ogawa, K. *Macromolecules* **1997**, *30*, 5849.
36. Magon, A.; Pyda, M. *Carbohydr. Res.* **2011**, *346*, 2558.
37. Ong, Y. T.; Ahmad, A. L.; Sharif Zein, S. H.; Sudesh, K.; Tan, S. H. *Sep. Purif. Technol.* **2011**, *76*, 419.
38. López, F. A.; Mercê, A. L. R.; Alguacil, F. J.; López-Delgado, A. *J. Therm. Anal. Calorim.* **2008**, *91*, 633.
39. Salam, M. A.; Makki, M. S. I.; Abdelaal, M. Y. A. *J. Alloys Compd.* **2011**, *509*, 2582.
40. Leerahawong, A.; Tanaka, M.; Okazaki, E.; Osako, K. *Fish Sci.* **2011**, *77*, 1061.
41. Wang, S. F.; Shen, L.; Zhang, W. D.; Tong, Y. *J. Biomacromolecules* **2005**, *6*, 3067.
42. Sun, F.; Cha, H. R.; Bae, K.; Hong, S.; Kim, J. M.; Kim, S. H.; Lee, J.; Lee, D. *Mater. Sci. Eng. A* **2011**, *528*, 6636.